



HAL
open science

Contrasted viral communities between *Aedes albopictus* and *Culex quinquefasciatus* in La Réunion Island

Sarah François, Aymeric Antoine-Lorquin, Doriane Mutuel, Patrick Makoundou, Marco Perriat-Sanguinet, Sandra Unal, Hélène Sobry, Anne-Sophie Gosselin-Grenet, Mylène Ogliastro, Mathieu Sicard, et al.

► To cite this version:

Sarah François, Aymeric Antoine-Lorquin, Doriane Mutuel, Patrick Makoundou, Marco Perriat-Sanguinet, et al.. Contrasted viral communities between *Aedes albopictus* and *Culex quinquefasciatus* in La Réunion Island. 2024. hal-04777812

HAL Id: hal-04777812

<https://hal.inrae.fr/hal-04777812v1>

Preprint submitted on 12 Nov 2024

HAL is a multi-disciplinary open access archive for the deposit and dissemination of scientific research documents, whether they are published or not. The documents may come from teaching and research institutions in France or abroad, or from public or private research centers.

L'archive ouverte pluridisciplinaire **HAL**, est destinée au dépôt et à la diffusion de documents scientifiques de niveau recherche, publiés ou non, émanant des établissements d'enseignement et de recherche français ou étrangers, des laboratoires publics ou privés.



Distributed under a Creative Commons Attribution - NonCommercial - NoDerivatives 4.0 International License

1
2 **Contrasted viral communities between *Aedes albopictus* and *Culex quinquefasciatus* in La**
3 **Réunion Island**

4
5
6 François S.^{1,2}, Antoine-Lorquin A.¹, Mutuel D.¹, Makoundou P.³, Perriat-Sanguinet M.³, Unal
7 S.³, Sobry H.¹, Gosselin-Grenet A.S.¹, Ogliastro M.¹, Sicard M.³, Weill M.³, Atyame C.⁴ &
8 Boëte C.^{3*}

9
10
11
12 ¹ DGIMI, Univ Montpellier, INRAE, Montpellier, France

13 ² Department of Biology, University of Oxford, South Park Road, Oxford, OX1 3SY, UK

14 ³ ISEM, Univ Montpellier, CNRS, IRD, EPHE, Montpellier 34095, France

15 ⁴ Université de La Réunion, UMR PIMIT (Processus Infectieux en Milieu Insulaire Tropical) CNRS
16 9192, INSERM 1187, IRD 249, Saint-Denis, île de La Réunion, France

17
18 *: corresponding author: christophe.boete@umontpellier.fr

19
20
21 **Abstract**

22
23 Mosquitoes are major vectors of arboviruses, and host a wide diversity of insect viruses.
24 Recent studies highlighted the impacts of mosquito-associated insect-specific viruses on the
25 transmission of arboviruses. However, we still lack knowledge on the biotic and abiotic factors
26 impacting the distribution dynamics of mosquito specific viruses, although such information
27 has the potential to inform arbovirus surveillance efforts. To gain knowledge on the
28 distribution of mosquito viruses in islands, we collected 13 *Aedes albopictus* and 9 *Culex*
29 *quinquefasciatus* pooled larvae samples in the Réunion Island, described their whole viral
30 communities at the family level by a viromic approach, and tested the impacts of mosquito
31 species and spatial distance on the structure of their viral communities.

32 Our study show that the composition of viral communities is more strongly linked to mosquito
33 species than to the geographic origin of samples. Spatial disparities were only observed in
34 *Aedes albopictus* viromes. Finally, we described the genomes of five virus taxa (an iflavivirus, an
35 ambidensovirus and three potentially novel microvirus species). Notably, we detected the
36 presence of a mosquito-infecting ambidensovirus, named CpDV, in *Aedes albopictus*. It was
37 previously only reported in *Culex pipiens*, implying that this densovirus may have a broader
38 host range than currently estimated.

39 Overall these results bring insights into the diversity and the distribution of mosquito viruses;
40 their unexplored interactions with two major vectors of arboviral diseases warrant further
41 studies.

42
43 **Keywords:**

44
45 Mosquito, viral metagenomics, virus diversity, virus surveillance, virus discovery

46
47 **1. Introduction**

48
49 Given their increasing global importance in public health issues, the understanding of viruses
50 infecting mosquitoes is largely biased toward the ones that have a medical or veterinary
51 importance. However, this has started to change with the progress of metagenomics that
52 permits to better apprehend the diversity of insect viromes (i.e. viral communities inferred by
53 viral genomic sequences). Apart from the fundamental interest to better understand the host-
54 parasite interactions between mosquitoes and the viruses infecting them, such approach are
55 considered of interest for zoonotic disease control (Olmo et al., 2023). Studies of the mosquito
56 virome allow to better estimate the diversity and the role of viruses in mosquito population
57 dynamics, their impact on the mosquito immune system and overall how their interactions
58 with arboviruses could eventually affect the epidemiology of the latter ones (Altinli et al.,
59 2021). Among the newly discovered viruses, a significant proportion are considered as insect-
60 specific viruses (ISV) and they are suspected to play a role in the transmission of arboviruses
61 in the case of coinfection (Wei et al., 2006; Bolling et al., 2012; Hobson-Peters et al., 2013;
62 Goenaga et al., 2015; Brinkmann, Nitsche and Kohl, 2016; Hall-Mendelin et al., 2016). This
63 potential role in modulating the transmission of pathogenic viruses highlights perspectives for
64 their eventual use as tools against arboviruses in the future (Agboli et al., 2019).

65 Despite the interest of discovering novel viruses from mosquitoes, metagenomic studies are
66 often restricted to making inventories of the discovered viruses and, apart from a recent work
67 (Pan et al., 2024), the majority of them do not address whether host taxonomy or spatial
68 distance may constrain the geographical distribution of these newly discovered mosquito
69 viruses, although such information has the potential to inform arbovirus surveillance efforts.
70 Our study has attempted to overcome this limitation. Our objective was to gain knowledge on
71 the factors impacting the circulation of mosquito viruses on the scale of an island. We tested
72 the relative impacts of mosquito species and spatial distance on the structure of mosquito-
73 associated viral communities. We focussed on two mosquito species that live in sympatry in
74 Réunion Island (Boussès et al., 2013): *Culex quinquefasciatus* and *Aedes albopictus*.

75 *Culex quinquefasciatus*, a member of the *Culex pipiens* species complex, is a vector of parasites
76 such as *Wuchereria bancrofti* and the avian malaria parasite *Plasmodium relictum*, but also of
77 arboviruses such as Rift Valley fever virus, West Nile virus and Saint-Louis encephalitis virus.
78 *C. quinquefasciatus* is distributed in tropical and subtropical regions worldwide (Samy et al.,
79 2016). *Aedes albopictus* is an invasive species native from South East Asia, distributed in the
80 intertropical areas and has spread in worldwide temperate regions (Kraemer et al., 2015) and
81 it is a vector of several arboviruses such as dengue, Zika or chikungunya.

82 We obtained viral communities associated with 22 samples of *A. albopictus* and *C.*
83 *quinquefasciatus* mosquitoes larvae that we sampled respectively in 13 and 9 locations on
84 both the windward (east) and leeward (west) sides of Réunion Island. This island, located in
85 the Indian Ocean, is characterised by a humid tropical climate and has been hit by a serious
86 outbreak of Chikungunya in 2005/2006 (Josseran et al., 2006). Chikungunya disease is still
87 present in Réunion Island in 2024, where dengue is also becoming endemic (Hafsia et al.,
88 2022; Vincent et al., 2023).

89

90 **2. Material and Methods**

91

92 *2.1. Sampling of Aedes albopictus and Culex quinquefasciatus populations*

93

94 Larvae of *A. albopictus* and *C. quinquefasciatus* were collected between February and April
95 2019 in 14 larvae breeding sites across Réunion Island (Fig. 1). Morphological characteristics
96 (body shape, siphon, antennae) were used for species identification. Almost all sites (except
97 the Sainte-Marie Ravine site) were cemeteries, corresponding to artificial breeding sites,
98 where mosquito larvae grow in flower pots that are regularly supplied with water (Table 1).
99 For each site and for each species, a batch of larvae was collected, rinsed several times with
100 tap water and larvae were sorted according to their species. Samples were then kept in
101 Eppendorf tubes and transported on ice to the lab then stored at -80°C until processing. Each
102 sample was a pool of larvae (stage L3/L4) and weighted between 1.17g and 1.49g for *A.*
103 *albopictus* and between 0.5g and 1.42g for *C. quinquefasciatus* (Table 1). Both mosquito
104 species were in sympatry in 8 sites, *A. albopictus* was found alone in 5 sites and *C.*
105 *quinquefasciatus* was alone in one site (Fig. 1).

106
107

108 2.2. Sample preparation and sequencing

109

110 Viromes were obtained from 22 mosquito samples (Table 1) as described in (François et al.,
111 2018). Briefly, $1.35\text{ g} \pm 0.1$ of material per sample of *A. albopictus* and $1.1\text{ g} \pm 0.3$ of material
112 per sample for *C. quinquefasciatus* was processed using a virion-associated nucleic acid
113 (VANA) based metagenomics approach to screen for the presence of both DNA and RNA
114 viruses. Samples were grounded and centrifuged to recover supernatants that were filtered
115 through a $0.45\ \mu\text{m}$ filter and centrifuged at $140,000\text{ g}$ for 2.5 hours to concentrate viral
116 particles. The resulting pellets were resuspended, and nucleic acids not protected in virus-like
117 particles (VLPs) were degraded by DNase and RNase incubation at 37°C for 1.5 h. Total RNA
118 and DNA were then extracted using a NucleoSpin kit (Macherey Nagel, Bethlehem, PA, USA)
119 following manufacturer's instructions. Reverse transcription was performed by SuperScript III
120 reverse transcriptase (Invitrogen), cDNAs were purified by a QIAquick PCR Purification Kit
121 (Qiagen, Hilden, Germany) and complementary strands synthesised by Klenow DNA
122 polymerase I. Double-stranded DNA was amplified by random PCR amplification. Samples
123 were barcoded during reverse transcription and PCR steps using homemade 26-nt Dodeca
124 Linkers coupled to homemade complementary PCR multiplex identifier primers. PCR products
125 were purified using NucleoSpin gel and PCR clean-up kit (Macherey Nagel, Bethlehem, PA,
126 USA) following manufacturer's instructions. Finally, libraries were prepared using NEBNext
127 Ultra DNA PCR free with Illumina adapter kit without fragmentation step from purified
128 amplicons and sequenced on an Illumina HiSeq 3000 to generate $2 \times 150\text{bp}$ paired-end reads
129 (Genewiz, South Plainfield, NJ, USA).

130

131 2.3. Viral Sequence analysis and Genome reconstruction

132

133 Illumina adaptors were removed and reads were filtered for quality (q30 quality and read
134 length $>45\text{ nt}$) using cutadapt 2.19 (Martin, 2011). Cleaned reads were assembled *de novo* into
135 contigs using MEGAHIT 1.2.9 (Li et al., 2015). Taxonomic assignment was achieved on contigs
136 of length $>900\text{ nt}$ through searches against the NCBI gbvrl viral database (created on
137 07/07/2021) using DIAMOND 0.9.30 with an e-value cutoff of $<10^{-3}$ (Buchfink et al., 2015). All
138 contigs that matched virus sequences were selected and used as queries to perform reciprocal
139 searches on NCBI non-redundant protein sequence database (created on July 2020) with an
140 e-value cutoff of $<10^{-3}$ in order to eliminate false positives.

141 Viral contigs completion and coverage was assessed by iterative mapping using Bowtie2 3.5.1
142 with the options end-to-end and very-sensitive (Langmead, 2010). Putative Open Reading
143 Frames (ORFs) were identified using ORF finder (length cutoff >400 nt) on Geneious prime
144 2021.1.1 (Kearse et al., 2012). Microviruses genome circularisation was performed using
145 Simple-Circularise 1.0 script (<https://github.com/Kzra/Simple-Circularise>) with minimal
146 overlap length of 20nt, and genome coverage was assessed by iterative mapping using
147 Bowtie2 3.5.1 with end-to-end sensitive options (Langmead, 2010). ORFs were annotated by
148 blastn query-centred alignment against the complete NCBI RefSeq viral database (created on
149 23/04/2021). Viral genomes completion was verified manually by aligning them to their 10
150 closest relatives downloaded from the GenBank nucleotide database (nr). In all subsequent
151 analyses, we focused only on full coding sequences (100% of CDS) based on the alignments of
152 genomes with their closest relatives combined with ORF completeness, thus discarding
153 contigs with partial CDS. The viral isolates that belonged to already described species were
154 reconstructed as follows: after mapping against the closest relative deposited in the NCBI
155 nucleotide database, consensus sequences were generated using samtools 1.2 (Danecek et
156 al., 2021). Mutations were called at depth ≥ 5 if they differed from the reference isolate;
157 otherwise, sites were kept as those of the reference isolate.

158

159 2.4. Viral Discovery and Taxonomic Assignment

160

161 To determine if viral contigs belonged to new species, their nucleotide sequences or their
162 predicted protein sequences were aligned and compared with the 10 closest related viral
163 genomes found by similarity searches performed above using MAFFT 7.450 with the G-INS-i
164 algorithm (Katoh et al., 2002; Katoh & Standley, 2013) or MUSCLE 3.8.425 (16 iterations)
165 (Edgar, 2004) using default settings. Genomes were classified as new virus strain or new virus
166 species according to the species demarcation thresholds recommended within the online
167 reports of the International Committee on Taxonomy of Virus (ICTV, <https://ictv.global/>).

168

169 2.5. Phylogenetic Analyses

170

171 Phylogenetic trees were built using Maximum Likelihood methods for all reconstructed full-
172 length CDS genomes in order to place them within the currently known viral diversity and to
173 infer their possible host range. Representative sets of replication-associated and capsid
174 proteins, or polyproteins, were extracted from the NCBI GenBank non-redundant (nr)
175 database for each taxonomic group in which the genomes were classified, comprising all the
176 ICTV ratified species and the 10 closest relatives found by blastx search against GenBank nr
177 DB on 27/06/2024, except for the *Densovirinae* phylogenetic tree that was based on all the
178 *Protoambidensovirus dipteran1* lineages.

179 Viral nucleotide sequences were aligned using MAFFT (option G-INS-i). Phylogenetic trees
180 were constructed in RAxML 8.2.11 (Stamatakis, 2014) using the GTR +GAMMA + I nucleotide
181 evolution model. Amino acid sequences were aligned using MUSCLE 5.1 (PPP algorithm) with
182 default settings. Sequences that were not reliably aligned due to high amino acid divergence
183 were removed and the dataset subsequently realigned. Phylogenetic trees were constructed
184 in RAxML 8.2.11 (Stamatakis, 2014) using the LG+I+G protein evolution model. Tree branch
185 support was estimated using 100 bootstrapped replicates. The trees were mid-point rooted
186 and visualised with MEGAX 10.2.4 (Stecher et al., 2020).

187

188 2.6. Statistical Analyses

189

190 Statistical analyses were performed using R and RStudio version 1.1.456 softwares (R Core
191 Team, 2023). Data from contingency tables were standardised to allow inter-sample
192 comparisons: taxonomic binning artefacts and potential inter-sample contamination were
193 restricted by applying an abundance threshold $>1/100,000$ reads/taxon/sample, and, for taxa
194 that contaminated negative controls, by removing them from sample datasets where their
195 abundance was equal or inferior to their abundance in controls (i.e. the number of reads
196 associated to a given family had to be above a threshold of 800 reads corresponding to the
197 background noise that was detected in the negative control).

198 To enable comparison between viral taxa that have different genome lengths, the number of
199 virus reads was divided by the length of the viral contig to which it mapped (kb). Viral diversity
200 accumulation curves in mosquito viromes were made using the Vegan package (vegan, 2012).
201 All the following analyses on virus community richness and composition were conducted at
202 the viral family level. The impact of host species on viral community α -diversity was evaluated
203 using the Shannon and Simpson diversity indices, and on β -diversity using Bray-Curtis
204 dissimilarity index. Differences in viromes structure of *A. albopictus* and *C. quinquefasciatus*
205 were visualised using a heatmap (“ggplot2: Elegant Graphics for Data Analysis (3e)”). The
206 effect of host species on viral communities was also determined by one-factor PERMANOVAs
207 with 10,000 permutations on Bray–Curtis matrix, using the adonis function of the VEGAN
208 package (Dixon, 2003). Permutational tests of dispersions (PERDISPs) using the function
209 permutest.betadisper (10000 permutations, pairwise) were performed to assess whether
210 significant effects could be influenced by differences in group dispersion (Anderson, 2001).
211 Statistical significance of PERMANOVA results was assumed when $p < 0.01$. The impact of host
212 species on viral abundance was assessed using Wilcoxon tests. Rare taxonomic groups
213 (occurring in <5 samples) were not considered for abundance analysis. Multiple comparison
214 test adjustment of p values was performed using the Benjamini-Yekutieli (BY) method
215 (Benjamini & Yekutieli, 2001). Finally, a potential correlation between sampling sites spatial
216 distances and virome composition was assessed by a Mantel test (10,000 random
217 permutations and Pearson correlation, package ade4 (Dray & Dufour, 2007)) on Bray-Curtis
218 virome beta diversity dissimilarity matrix.

219

220 3. Results

221

222 3.1. Viromes comparison between sympatric *Culex quinquefasciatus* and *Aedes albopictus*, 223 and virus spatial distribution in the Réunion island

224

225 The sequencing depth was sufficient to recover the entire viral communities at the family level
226 as indicated by the rarefaction curves (Fig. 2a). In addition, the accumulation curve (number
227 of taxa/number of samples) (Fig. 2b) revealed that our sampling effort permitted to recover
228 the entire diversity of viral families circulating in the targeted Culicidae samples.

229

230 We reconstructed 46 viral contigs (ST1) ranging from 314 to 10844 nt. The taxonomic
231 assignment of the contigs obtained from the 22 samples (13 *A. albopictus* samples and 9 *C.*
232 *quinquefasciatus* samples) to viral families was highly variables among samples, ranging
233 between 0 to 100 % with an average value of 59.61% of the total number of cleaned reads
234 assigned to viral contigs, the remaining reads not being classified (Fig. 3). This range of viral

235 read abundance is congruent with another recent insect viral metagenomic studies based on
236 the same protocol (François et al., 2021). We detected viral sequences that could not be
237 classified at the family level, as they belonged to unclassified virus clades. These unclassified
238 viral sequences were detected in all samples, with the exception of *C. quinquefasciatus* from
239 Saint-Benoît, and their abundance was higher (>90% reads) in *A. albopictus* from La Possession
240 and *C. quinquefasciatus* from Saint-Denis. As they could not be classified into existing families,
241 these sequences were not taken into account in further analyses.

242
243 Overall, we found 12 virus families (including 6 associated with *A. albopictus* and 9 with *C.*
244 *quinquefasciatus*) in the larvae pools (Fig. 4). Notably, a majority of families (8/12) have RNA
245 genomes. Among them, 2 families of positive single-stranded RNA viruses were known as
246 insect-specific viruses (*Dicistroviridae* and *Iflaviridae*); while only one of DNA viruses
247 (*Parvoviridae*) was known to infect insects (*Densovirinae* subfamily). Arthropod-infecting
248 viruses represented 67.9% of all reads, and the most represented families in term of read
249 abundance are *Parvoviridae* (single-stranded DNA virus, 44.7% of all virus reads) and
250 *Iflaviridae* (positive single-stranded RNA virus, 21.1% reads). Members of the *Phasmaviridae*
251 family (negative single-stranded RNA virus whose host range includes insects) are less
252 abundant (around 1% of the total number of reads in *Culex* samples), and were detected in 4
253 sites. Sequences related to bacteriophages families were also detected (*Microviridae*, ST2) and
254 account for 4.2% of the total viral reads.

255
256 *Culex* samples (mean number of viral reads: 96,296; min: 619 reads; max: 532,533 reads,
257 average percentage of viral reads: 4.2%) did not contain more virus reads than *Aedes* samples
258 (mean number of viral reads: 25,350; min: 727; max: 225,372, average percentage of viral
259 reads: 15.4%), Wilcoxon test p value = 0.14. Considering the most represented families in term
260 of occurrence, 92.1% of the reads are related to 5 families; and viruses of the family
261 *Parvoviridae* were found in 3 *Aedes* samples and in 2 *Culex* samples, while iflavirus reads were
262 detected in 5 *Aedes* samples and in 7 *Culex* samples (Fig. 4, ST2).

263
264 We then evaluated whether mosquito species could explain for differences in mosquito
265 viromes richness and composition. While we found no differences in Shannon and Simpson α -
266 diversity indices between mosquito species (SF1), MDS plot and PERMANOVAs based on Bray-
267 Curtis dissimilarity matrices showed significant differences in virus community composition
268 between mosquito species (p value = 0.0001 and R^2 = 17 %, Fig. 5). We conducted a
269 differential abundance analysis by Wilcoxon tests corrected by BY method for multiple
270 comparisons on viral families present in > 5 samples (i.e. *Iflaviridae*, *Microviridae*,
271 *Parvoviridae*, *Phasmaviridae*, *Phycoviridae*, *Rhabdoviridae* and *Siphoviridae* families) to assess
272 which viruses drove this observed difference (Fig. 6). Difference in community composition
273 was driven by *Microviridae* family members (bacteriophages) that were more abundant in *A.*
274 *albopictus* samples, and by insect-infecting viruses belonging to the *Phasmaviridae* and
275 *Rhabdoviridae* families which were more abundant in *C. quinquefasciatus* samples (adjusted
276 p value < 0.05).

277 Finally, we tested whether spatial distance between sampling locations could impact
278 mosquito viromes composition, by conducting a Mantel test using Pearson correlation based
279 on Bray-Curtis dissimilarity matrix and a pairwise distance matrix between sampling locations.

280 While Mantel test showed no significance for *C. quinquefasciatus* viromes, it showed a
281 negative correlation between geographical distance and viromes similarity for *A. albopictus*
282 samples (p value = 0.016, observed correlation: 31%).

283 Our study thus suggests that there were differences of virus distribution between the two
284 mosquito species, and spatial variation in *A. albopictus* viromes composition. Our results tend
285 to show that virome composition may be more explained by mosquito species than by spatial
286 distribution that may be linked to unmeasured ecological conditions (Fig. 5 and 6).

287

288 3.2. Virus discovery and phylogenetic analysis

289

290 Incomplete viral coding sequences (CDS) were discarded from the following analyses, as only
291 virus with complete CDS can be classified as belonging to new or already known species using
292 ICTV species demarcation criteria based on sequence data similarity to their closest relatives
293 (Simmonds *et al.*, 2017; Siddell *et al.*, 2023).

294 We reconstructed 5 viral full-length CDS or genomes. The coverage depth across all these
295 genomes is high (between 62 and 12,521) with read numbers ranging from 2,200 to 501,573
296 mapped reads per sample for each genome (Table 2). We built ML phylogenetic trees to place
297 these viruses within the currently known viral diversity and to infer their possible host range.

298

299 3.2.1. *Densovirinae*

300

301 *Densovirinae* is a subfamily of the *Parvoviridae* family whose members infect arthropods,
302 crustaceans and echinoderms (Cotmore *et al.*, 2014). We report the complete CDS of a
303 densovirus, named *Culex quinquefasciatus* associated densovirus isolate 2019_VP12-D87,
304 whose contig length is 5,459nt, and which shows 89.0% genome-wide nucleotide identity to
305 a *Dipteran protoambidensovirus 1* lineage isolated from *Culex pipiens* mosquitoes
306 (FJ810126.1, *Protoambidensovirus* genus, common virus name: *Culex pipiens* densovirus)
307 (Table 2). According to the species demarcation threshold in the *Densovirinae* subfamily (i.e.,
308 < 85% NS1 protein identity (Cotmore *et al.*, 2014)), this new genome (accession number:
309 PQ041300) thus represents a new distant lineage of *Dipteran protoambidensovirus*. The
310 position of our CpDV sequence in the NS1 gene tree shows that our lineage belongs to the
311 CpDV-3 clade which was previously only represented by sequences collected from Beijing
312 (China) samples in 2003 (Fig. 7) (Altinli *et al.*, 2019).

313

314 3.2.2. *Iflaviridae*

315

316 The *Iflaviridae* family comprises picorna-like viruses infecting arthropods. In our study we
317 found a novel iflavirus lineage which was detected in a pool of *C. quinquefasciatus* from Saint-
318 Benoît. We named it *Culex quinquefasciatus* associated iflavirus isolate Saint_Denis, whose
319 contig length is 10,074nt (Table 2, accession number: PQ041301). Its closed relative is the
320 *XiangYun picorna-like virus 4* species (Feng *et al.*, 2022) that was discovered in *Culex theileri*
321 from Yunnan, China (Iflavirus genus, accession number OL700176) with which it shared a
322 whole polyprotein pairwise identity of 98.5 (Table 2). The *Iflaviridae* species demarcation
323 criterion is set as < 90% of capsid proteins identity (Valles *et al.*, 2017). Our virus thus belongs
324 to the *XiangYun picorna-like virus 4* species, which may infect *Culex spp.* Finally, *Culex*
325 *quinquefasciatus* associated iflavirus isolate 2019_VP12-D85 clustered in a monophyletic

326 clade containing only viral taxa isolated from dipteran species (mosquitoes and true flies),
327 indicating that this lineage is likely specific of dipterans (Fig. 8).

328

329 3.2.3. *Microviridae*

330

331 We reconstructed 3 complete circularised genomes belonging to bacteriophages from the
332 *Microviridae* family (circular ssDNA viruses). Their similarity to already known microvirus
333 species is relatively low (54.5% to 75.0% of amino acid identity in major capsid and replication-
334 associated proteins) (Table 2). Thus, while there is currently no species demarcation criteria
335 based on genome similarity defined by the ICTV for the *Microviridae* family (Kirchberger &
336 Ochman, 2023), those 3 genomes could belong to novel viral species, tentatively named *Aedes*
337 *albopictus* associated microvirus 1, 2 and 3 (accession numbers: PQ041302, PQ041303 and
338 PQ041304, respectively). Those 3 microviruses cluster with members of the *Gokushovirinae*
339 subfamily that were isolated from water ecosystems (Fig. 9, Table 2).

340

341 4. Discussion

342

343 We studied the viromes of two mosquito species that are major vectors of arboviruses.
344 However, we did not detect any arboviruses in our screened larvae samples despite the
345 ongoing circulation of dengue in Réunion Island; this is explained by the fact that we studied
346 the virome isolated from larvae and not from adult mosquitoes and by the low level of vertical
347 transmission of arboviruses, which is typically between 0.1 and 4 % (Adams & Boots, 2010;
348 Lequime et al., 2016). Our study shows that, in the Réunion Island, patterns of mosquito-
349 associated virus distribution may be more explained by mosquito species rather than by
350 geographical location. Our results are congruent with those obtained from other viral
351 metagenomic studies (Sadeghi et al., 2018; Sanborn et al., 2019; Kubacki et al., 2020;
352 Thongsripong et al., 2021), which highlighted that virus distributions is correlated to the
353 mosquito taxonomy (Faizah et al., 2020), as shown previously in a metatranscriptomic study
354 conducted in China (Pan et al., 2024) and a shotgun sequencing study from Thailand
355 (Thongsripong et al., 2021).

356

357 We used a stringent threshold for virus detection, and thus only classified complete viral CDS
358 at the species level, in order to reduce the risk of false-positive detection errors, at the cost of
359 underestimating the number of virus taxa present in our viromes. However, we could
360 reconstruct the full-length genomes of three potential new bacteriophages species belonging
361 to the *Microviridae* family. Their specifically high abundance in *Aedes* samples suggests that
362 they may infect *Aedes albopictus* larvae microbiota, although their presence could also be due
363 to environmental or diet contamination by infected aquatic bacteria. However their absence
364 or low abundance in the *Culex* samples (some of them sharing the same breeding sites with
365 the *Aedes*) tends to favour the idea of an association with *Aedes albopictus*.

366 We also reported the full CDS of a divergent insect-infecting iflavirus lineage belonging to the
367 *XiangYun picorna-like virus 4* species. This iflavirus clustered in a monophyletic clade
368 containing only viral taxa isolated from dipteran species (mosquitoes and true flies), and was
369 previously reported by Feng et al. in *Culex theileri* in China (Feng et al., 2022). Altogether,
370 these results indicate that this virus is probably common in *Culex spp.* Further work is needed
371 to determine the prevalence of XiangYun picorna-like virus 4 in natural populations of
372 mosquitoes and its eventual impact on mosquito fitness.

373 Interestingly, we finally reported for the first time the presence of *Dipteran*
374 *protoambidensovirus 1* (common name: *Culex pipiens* densovirus, clade CpDV-3), a mosquito-
375 infecting ambidensovirus, in *A. albopictus*. Reported CpDV host range currently only includes
376 *Culex pipiens* (Altinli et al., 2019, 2020), its broadening to *A. albopictus* species warrants
377 further confirmation, as a broader host range likely impacts CpDV evolution.
378

379 Data availability statement

380 The genomic sequences of the five full-length viral genomes or CDS have been deposited at
381 GenBank under the accession numbers PQ041300 to PQ041304. High-throughput sequencing
382 reads were deposited in SRA under the accession no. SRR29133481 to SRR29133504 under
383 PRJNA1114772 BioProject. The bioinformatics pipeline code is available at
384 <https://github.com/ayantoine/NearVANA>.

385

386 References

387

388 Adams, B., Boots, M. (2010). How important is vertical transmission in mosquitoes for the
389 persistence of dengue? Insights from a mathematical model. *Epidemics*, 2, 1–10.
390 <https://doi.org/10.1016/j.epidem.2010.01.001>

391 Agboli, E., Leggewie, M., Altinli, M., Schnettler, E. (2019). Mosquito-specific viruses—
392 transmission and interaction. *Viruses*, 11, 873. <https://doi.org/10.3390/v11090873>

393 Altinli, M., Lequime, S., Atyame, C., Justy, F., Weill, M., Sicard, M. (2020). Wolbachia modulates
394 prevalence and viral load of *Culex pipiens* densoviruses in natural populations. *Molecular*
395 *Ecology*, 29, 4000–4013. <https://doi.org/10.1111/mec.15609>

396 Altinli, M., Lequime, S., Courcelle, M., François, S., Justy, F., Gosselin-Grenet, A.-S., Ogliastro,
397 M., Weill, M., Sicard, M. (2019). Evolution and phylogeography of *Culex pipiens* densovirus.
398 *Virus Evolution*, 5, vez053. <https://doi.org/10.1093/ve/vez053>

399 Altinli, M., Schnettler, E., Sicard, M. (2021). Symbiotic interactions between mosquitoes and
400 mosquito viruses. *Frontiers in Cellular and Infection Microbiology*, 11.
401 <https://doi.org/10.3389/fcimb.2021.694020>

402 Anderson, M.J. (2001). A new method for non-parametric multivariate analysis of variance.
403 *Austral Ecology*, 26, 32–46. <https://doi.org/10.1111/j.1442-9993.2001.01070.pp.x>

404 Benjamini, Y., Yekutieli, D. (2001). The control of the false discovery rate in multiple testing
405 under dependency. *The Annals of Statistics*, 29, 1165–1188.
406 <https://doi.org/10.1214/aos/1013699998>

407 Bolling, B.G., Olea-Popelka, F.J., Eisen, L., Moore, C.G., Blair, C.D. (2012). Transmission
408 dynamics of an insect-specific flavivirus in a naturally infected *Culex pipiens* laboratory colony
409 and effects of co-infection on vector competence for West Nile virus. *Virology*, 427, 90–97.
410 <https://doi.org/10.1016/j.virol.2012.02.016>

411 Bousès, P., Dehecq, J.S., Brengues, C., Fontenille, D. (2013). Inventaire actualisé des
412 moustiques (Diptera: Culicidae) de l'île de La Réunion, océan Indien. *Bulletin de la Société de*
413 *pathologie exotique*, 106, 113–125. <https://doi.org/10.1007/s13149-013-0288-7>

414 Brinkmann, A., Nitsche, A., Kohl, C. (2016). Viral metagenomics on blood-feeding arthropods
415 as a tool for human disease surveillance. *International Journal of Molecular Sciences*, 17, 1743.
416 <https://doi.org/10.3390/ijms17101743>

- 417 Buchfink, B., Xie, C., Huson, D.H. (2015). Fast and sensitive protein alignment using DIAMOND.
418 *Nature Methods*, 12, 59–60. <https://doi.org/10.1038/nmeth.3176>
- 419 Capella-Gutiérrez, S., Silla-Martínez, J.M., Gabaldón, T. (2009). trimAl: a tool for automated
420 alignment trimming in large-scale phylogenetic analyses. *Bioinformatics*, 25, 1972–1973.
421 <https://doi.org/10.1093/bioinformatics/btp348>
- 422 Cotmore, S.F., Agbandje-McKenna, M., Chiorini, J.A., Mukha, D.V., Pintel, D.J., Qiu, J.,
423 Soderlund-Venermo, M., Tattersall, P., Tijssen, P., Gatherer, D., Davison, A.J. (2014). The
424 family Parvoviridae. *Archives of Virology*, 159, 1239–1247. <https://doi.org/10.1007/s00705-013-1914-1>
- 425
426 Danecek, P., Bonfield, J.K., Liddle, J., Marshall, J., Ohan, V., Pollard, M.O., Whitwham, A.,
427 Keane, T., McCarthy, S.A., Davies, R.M., Li, H. (2021). Twelve years of SAMtools and BCFtools.
428 *GigaScience*, 10, giab008. <https://doi.org/10.1093/gigascience/giab008>
- 429 Dixon, P. (2003). VEGAN, a package of R functions for community ecology. *Journal of*
430 *Vegetation Science*, 14, 927–930. <https://doi.org/10.1111/j.1654-1103.2003.tb02228.x>
- 431 Dray, S., Dufour, A.-B. (2007). The ade4 Package: Implementing the Duality Diagram for
432 Ecologists. *Journal of Statistical Software*, 22, 1–20. <https://doi.org/10.18637/jss.v022.i04>
- 433 Edgar, R.C. (2004). MUSCLE: multiple sequence alignment with high accuracy and high
434 throughput. *Nucleic Acids Research*, 32, 1792–1797. <https://doi.org/10.1093/nar/gkh340>
- 435 ☐ Faizah, A. N., Kobayashi, D., Isawa, H., Amoa-Bosompem, M., Murota, K., Higa, Y., Futami,
436 K., Shimada, S., Kim, K. S., Itokawa, K., Watanabe, M., Tsuda, Y., Minakawa, N., Miura, K.,
437 Hirayama, K., & Sawabe, K. (2020). Deciphering the virome of *Culex vishnui* subgroup
438 mosquitoes, the major vectors of Japanese encephalitis, in Japan. *Viruses*, 12, 264.
439 <https://doi.org/10.3390/v12030264>
- 440 ☐ Feng, Y., Gou, Q.-Y., Yang, W.-H., Wu, W.-C., Wang, J., Holmes, E. C., Liang, G., & Shi, M.
441 (2022). A time-series meta-transcriptomic analysis reveals the seasonal, host, and gender
442 structure of mosquito viromes. *Virus Evolution*, 8, veac006.
443 <https://doi.org/10.1093/ve/veac006>
- 444 ☐ François, S., Antoine-Lorquin, A., Kulikowski, M., Frayssinet, M., Filloux, D., Fernandez, E.,
445 Roumagnac, P., Froissart, R., & Ogliastro, M. (2021). Characterisation of the viral community
446 associated with the alfalfa weevil (*Hypera postica*) and its host plant, alfalfa (*Medicago sativa*).
447 *Viruses*, 13, 791. <https://doi.org/10.3390/v13050791>
- 448 ☐ François, S., Filloux, D., Fernandez, E., Ogliastro, M., & Roumagnac, P. (2018). Viral
449 metagenomics approaches for high-resolution screening of multiplexed arthropod and plant
450 viral communities. In Pantaleo, V. & Chiumenti, M. (Eds.), *Viral Metagenomics: Methods and*
451 *Protocols* (pp. 77–95). Springer, New York, NY. https://doi.org/10.1007/978-1-4939-7683-6_7
- 452 ☐ Goenaga, S., Kenney, J. L., Duggal, N. K., Delorey, M., Ebel, G. D., Zhang, B., Levis, S. C., Enria,
453 D. A., & Brault, A. C. (2015). Potential for co-infection of a mosquito-specific flavivirus,
454 Nhumirim virus, to block West Nile virus transmission in mosquitoes. *Viruses*, 7, 5801–5812.
455 <https://doi.org/10.3390/v7112911>
- 456 ☐ Hafsia, S., Haramboure, M., Wilkinson, D. A., Baldet, T., Yemadje-Menudier, L., Vincent, M.,
457 Tran, A., Atyame, C., & Mavingui, P. (2022). Overview of dengue outbreaks in the
458 southwestern Indian Ocean and analysis of factors involved in the shift toward endemicity in
459 Reunion Island: A systematic review. *PLOS Neglected Tropical Diseases*, 16, e0010547.
460 <https://doi.org/10.1371/journal.pntd.0010547>
- 461 ☐ Hall, R. A., Bielefeldt-Ohmann, H., McLean, B. J., O'Brien, C. A., Colmant, A. M. G., Piyasena,
462 T. B. H., Harrison, J. J., Newton, N. D., Barnard, R. T., Prow, N. A., Deerain, J. M., Mah, M. G. K.
463 Y., & Hobson-Peters, J. (2016). Commensal viruses of mosquitoes: Host restriction,

464 transmission, and interaction with arboviral pathogens. *Evolutionary Bioinformatics*, 12s2,
465 EBO.S40740. <https://doi.org/10.4137/EBO.S40740>

466 ▣ Hobson-Peters, J., Yam, A. W. Y., Lu, J. W. F., Setoh, Y. X., May, F. J., Kurucz, N., Walsh, S.,
467 Prow, N. A., Davis, S. S., Weir, R., Melville, L., Hunt, N., Webb, R. I., Blitvich, B. J., Whelan, P.,
468 & Hall, R. A. (2013). A new insect-specific flavivirus from Northern Australia suppresses
469 replication of West Nile virus and Murray Valley encephalitis virus in co-infected mosquito
470 cells. *PLOS ONE*, 8, e56534. <https://doi.org/10.1371/journal.pone.0056534>

471 ▣ Jossieran, L., Paquet, C., Zehgnoun, A., Caillere, N., Le Tertre, A., Solet, J.-L., & Ledrans, M.
472 (2006). Chikungunya disease outbreak, Reunion Island. *Emerging Infectious Diseases*, 12,
473 1994–1995. <https://doi.org/10.3201/eid1212.060710>

474 ▣ Katoh, K., Misawa, K., Kuma, K., & Miyata, T. (2002). MAFFT: a novel method for rapid
475 multiple sequence alignment based on fast Fourier transform. *Nucleic Acids Research*, 30,
476 3059–3066. <https://doi.org/10.1093/nar/gkf436>

477 Katoh K, Standley DM (2013) MAFFT Multiple Sequence Alignment Software Version 7:
478 Improvements in Performance and Usability. *Molecular Biology and Evolution* 30, 772–780.
479 <https://doi.org/10.1093/molbev/mst010>

480 Kearse M, Moir R, Wilson A, Stones-Havas S, Cheung M, Sturrock S, Buxton S, Cooper A,
481 Markowitz S, Duran C, Thierer T, Ashton B, Meintjes P, Drummond A (2012) Geneious Basic:
482 an integrated and extendable desktop software platform for the organization and analysis of
483 sequence data. *Bioinformatics* 28, 1647–1649.
484 <https://doi.org/10.1093/bioinformatics/bts199>

485 Kirchberger PC, Ochman H (2023) Microviruses: A World Beyond phiX174. *Annual Review of*
486 *Virology* 10, 99–118. <https://doi.org/10.1146/annurev-virology-100120-011239>

487 Kraemer MUG, Sinka ME, Duda KA, Mylne AQN, Shearer FM, Barker CM, Moore CG, Carvalho
488 RG, Coelho GE, Van Bortel W, Hendrickx G, Schaffner F, Elyazar IRF, Teng H-J, Brady OJ,
489 Messina JP, Pigott DM, Scott TW, Smith DL, Wint GRW, Golding N, Hay SI (2015) The global
490 distribution of the arbovirus vectors *Aedes aegypti* and *Ae. albopictus*. *eLife* 4, e08347.
491 <https://doi.org/10.7554/eLife.08347>

492 Kubacki J, Flacio E, Qi W, Guidi V, Tonolla M, Fraefel C (2020) Viral Metagenomic Analysis of
493 *Aedes albopictus* Mosquitos from Southern Switzerland. *Viruses* 12, 929.
494 <https://doi.org/10.3390/v12090929>

495 Langmead B (2010) Aligning Short Sequencing Reads with Bowtie. *Current Protocols in*
496 *Bioinformatics* 32, 11.7.1-11.7.14. <https://doi.org/10.1002/0471250953.bi1107s32>

497 Lequime S, Paul RE, Lambrechts L (2016) Determinants of Arbovirus Vertical Transmission in
498 Mosquitoes. *PLOS Pathogens* 12, e1005548. <https://doi.org/10.1371/journal.ppat.1005548>

499 Li D, Liu C-M, Luo R, Sadakane K, Lam T-W (2015) MEGAHIT: an ultra-fast single-node solution
500 for large and complex metagenomics assembly via succinct de Bruijn graph. *Bioinformatics* 31,
501 1674–1676. <https://doi.org/10.1093/bioinformatics/btv033>

502 Martin M (2011) Cutadapt removes adapter sequences from high-throughput sequencing
503 reads. *EMBnet journal* 17, 10–12. <https://doi.org/10.14806/ej.17.1.200>

504 Olmo RP, Todjro YMH, Aguiar ERGR, de Almeida JPP, Ferreira FV, Armache JN, de Faria IJS,
505 Ferreira AGA, Amadou SCG, Silva ATS, de Souza KPR, Vilela APP, Babarit A, Tan CH, Diallo M,
506 Gaye A, Paupy C, Obame-Nkoghe J, Visser TM, Koenraadt CJM, Wongsokarijo MA, Cruz ALC,
507 Prieto MT, Parra MCP, Nogueira ML, Avelino-Silva V, Mota RN, Borges MAZ, Drummond BP,
508 Kroon EG, Recker M, Sedda L, Marois E, Imler J-L, Marques JT (2023) Mosquito vector
509 competence for dengue is modulated by insect-specific viruses. *Nature Microbiology* 8, 135–
510 149. <https://doi.org/10.1038/s41564-022-01289-4>

- 511 Pan Y-F, Zhao H, Gou Q-Y, Shi P-B, Tian J-H, Feng Y, Li K, Yang W-H, Wu D, Tang G, Zhang B,
512 Ren Z, Peng S, Luo G-Y, Le S-J, Xin G-Y, Wang J, Hou X, Peng M-W, Kong J-B, Chen X-X, Yang C-
513 H, Mei S-Q, Liao Y-Q, Cheng J-X, Wang J, Chaolemen, Wu Y-H, Wang J-B, An T, Huang X, Eden
514 J-S, Li J, Guo D, Liang G, Jin X, Holmes EC, Li B, Wang D, Li J, Wu W-C, Shi M (2024) Metagenomic
515 analysis of individual mosquito viromes reveals the geographical patterns and drivers of viral
516 diversity. *Nature Ecology & Evolution* 8, 947–959. [https://doi.org/10.1038/s41559-024-](https://doi.org/10.1038/s41559-024-02365-0)
517 [02365-0](https://doi.org/10.1038/s41559-024-02365-0)
- 518 R Core Team (2023) *R: A Language and Environment for Statistical Computing*.
- 519 Sadeghi M, Altan E, Deng X, Barker CM, Fang Y, Coffey LL, Delwart E (2018) Virome of > 12
520 thousand *Culex* mosquitoes from throughout California. *Virology* 523, 74–88.
521 <https://doi.org/10.1016/j.virol.2018.07.029>
- 522 Samy AM, Elaagip AH, Kenawy MA, Ayres CFJ, Peterson AT, Soliman DE (2016) Climate Change
523 Influences on the Global Potential Distribution of the Mosquito *Culex quinquefasciatus*, Vector
524 of West Nile Virus and Lymphatic Filariasis. *PLOS ONE* 11, e0163863.
525 <https://doi.org/10.1371/journal.pone.0163863>
- 526 Sanborn MA, Klein TA, Kim H-C, Fung CK, Figueroa KL, Yang Y, Asafo-adjei EA, Jarman RG, Hang
527 J (2019) Metagenomic Analysis Reveals Three Novel and Prevalent Mosquito Viruses from a
528 Single Pool of *Aedes vexans nipponii* Collected in the Republic of Korea. *Viruses* 11, 222.
529 <https://doi.org/10.3390/v11030222>
- 530 Siddell SG, Smith DB, Adriaenssens E, Alfenas-Zerbini P, Dutilh BE, Garcia ML, Junglen S,
531 Krupovic M, Kuhn JH, Lambert AJ, Lefkowitz EJ, Łobocka M, Mushegian AR, Oksanen HM,
532 Robertson DL, Rubino L, Sabanadzovic S, Simmonds P, Suzuki N, Van Doorslaer K, Vandamme
533 A-M, Varsani A, Zerbini FM (2023) Virus taxonomy and the role of the International Committee
534 on Taxonomy of Viruses (ICTV). *The Journal of General Virology* 104, 001840.
535 <https://doi.org/10.1099/jgv.0.001840>
- 536 Simmonds P, Adams MJ, Benkó M, Breitbart M, Brister JR, Carstens EB, Davison AJ, Delwart E,
537 Gorbalenya AE, Harrach B, Hull R, King AMQ, Koonin EV, Krupovic M, Kuhn JH, Lefkowitz EJ,
538 Nibert ML, Orton R, Roossinck MJ, Sabanadzovic S, Sullivan MB, Suttle CA, Tesh RB, van der
539 Vlugt RA, Varsani A, Zerbini FM (2017) Virus taxonomy in the age of metagenomics. *Nature*
540 *Reviews Microbiology* 15, 161–168. <https://doi.org/10.1038/nrmicro.2016.177>
- 541 Stamatakis A (2014) RAxML version 8: a tool for phylogenetic analysis and post-analysis of
542 large phylogenies. *Bioinformatics* 30, 1312–1313.
543 <https://doi.org/10.1093/bioinformatics/btu033>
- 544 Stecher G, Tamura K, Kumar S (2020) Molecular Evolutionary Genetics Analysis (MEGA) for
545 macOS. *Molecular Biology and Evolution* 37, 1237–1239.
546 <https://doi.org/10.1093/molbev/msz312>
- 547 Thongsripong P, Chandler JA, Kittayapong P, Wilcox BA, Kapan DD, Bennett SN (2021)
548 Metagenomic shotgun sequencing reveals host species as an important driver of virome
549 composition in mosquitoes. *Scientific Reports* 11, 8448. [https://doi.org/10.1038/s41598-021-](https://doi.org/10.1038/s41598-021-87122-0)
550 [87122-0](https://doi.org/10.1038/s41598-021-87122-0)
- 551
- 552 Valles SM, Chen Y, Firth AE, Guérin DMA, Hashimoto Y, Herrero S, de Miranda JR, Ryabov E,
553 ICTV Report Consortium (2017) ICTV Virus Taxonomy Profile: *Iflaviridae*. *Journal of General*
554 *Virology* 98, 527–528. <https://doi.org/10.1099/jgv.0.000757>
- 555 *vegan: Community Ecology Package* (2012).
- 556 Vincent M, Paty MC, Gerardin P, Balleydier E, Etienne A, Daoudi J, Thouillot F, Jaffar-Bandjee M-
557 C, Team CI, Network L, Réunion on behalf of the study collaborators Réseau de médecins
558 sentinelles de la, Menudier L (2023) From dengue outbreaks to endemicity: Reunion Island,

559 France, 2018 to 2021. *Eurosurveillance* 28, 2200769. [https://doi.org/10.2807/1560-](https://doi.org/10.2807/1560-7917.ES.2023.28.29.2200769)
560 [7917.ES.2023.28.29.2200769](https://doi.org/10.2807/1560-7917.ES.2023.28.29.2200769)

561 Wei W, Shao D, Huang X, Li J, Chen H, Zhang Q, Zhang J (2006) The pathogenicity of mosquito
562 densovirus (C6/36DENV) and its interaction with dengue virus type II in *Aedes albopictus*. *The*
563 *American Journal of Tropical Medicine and Hygiene* 75, 1118–1126.
564 <https://doi.org/10.4269/ajtmh.2006.75.1118>

565

566

567 **Acknowledgements**

568 We thank Yann Gomard, Cyrille Lebon and Sarah Hafsah for their help in collecting samples
569 in the field.

570

571 **Funding**

572 This work was funded by the French ANSES PNR EST programme (project 2018/1/183,
573 "DENSOTOOL," 2019–2023).

574

575 **Conflict of interest disclosure**

576 No financial conflicts of interest in relation to the content of the article.

577 **Figures**

578

579 **Figure 1:** Information on sampling locations on Reunion Island, Indian Ocean. Larvae from
580 different breeding sites have been pooled by sampling location. In some cases breeding sites
581 were hosting one or both of the species of interest.

582

583 **Figure 2: Viral communities recovery efforts. a.** Rarefaction curves of viral communities
584 recovered from mosquito samples at the family level. **b.** Accumulation curve of viral
585 communities recovered from mosquito samples at the family level.

586

587 **Figure 3:** Proportion of viral reads classified at the family level.

588 *Aedes albopictus* (red); *Culex quinquefasciatus* (blue).

589

590 **Figure 4:** Abundance of viruses found in *Aedes albopictus* (red) and *Culex quinquefasciatus*
591 (blue). The horizontal axis represents the log (1+ number of reads attributed to each family).
592 The number aside each dot represents the number of samples where the corresponding family
593 was found.

594

595 **Figure 5:** Non-metric multi-dimensional scaling (MDS) plot of virus communities based on
596 Bray-Curtis dissimilarity matrix, at the family level. A PERMANOVA, also based on Bray-Curtis
597 dissimilarity matrix and permutational tests of dispersions (PERDISPs) was conducted in
598 complement (R² value: 17%), with a *p* value <0.0001. Samples are coloured by host species.

599

600 **Figure 6:** Heatmap representing the abundance of virus families in *Aedes albopictus* and *Culex*
601 *quinquefasciatus* samples. The colours represent the normalised proportion of reads

602 attributed to each family. Sample names between ‘*’ correspond to *Aedes albopictus* while
603 others correspond to *Culex quinquefasciatus*.

604
605

606 **Figure 7:** Maximum likelihood phylogenetic tree based on the NS1 nucleotide sequences of 52
607 *Dipteran protoambidensovirus 1* (common virus name: *Culex pipiens densovirus* (CpDV))
608 sequences. The alignment of 892 nucleotides in length was produced by MAFFT v7.450 using
609 the G-INS-i algorithm. The tree is mid-point rooted. Bootstrap values (100 replicates) are
610 indicated at each node. Scale bar corresponds to nucleotide substitutions per site. The CpDV
611 sequence obtained from our samples is coloured in red. CpDV clades were defined according
612 to (Altinli et al., 2019).

613

614 **Figure 8:** Maximum likelihood phylogenetic tree based on the polyprotein amino acid
615 sequences of 27 *Iflaviridae* sequences. The alignment of 2102 amino acids in length was
616 produced by MUSCLE 5.1, and unconserved regions were trimmed by trimAL 1.4 using default
617 parameters (Capella-Gutiérrez et al., 2009). The tree is mid-point rooted. Bootstrap values
618 (100 replicates) are indicated at each node. Scale bar corresponds to amino acid substitutions
619 per site. The sequence obtained from our samples is coloured in red, and the blue sequences
620 represented viruses isolated from dipteran species.

621

622 **Figure 9:** Maximum likelihood phylogenetic tree based on the major capsid protein amino acid
623 sequences of 65 *Microviridae* sequences. The alignment of 487 amino acids in length was
624 produced by MUSCLE 5.1, and unconserved regions were trimmed by trimAL 1.4 using default
625 parameters (Capella-Gutiérrez et al., 2009). The tree is mid-point rooted. Bootstrap values
626 (100 replicates, ≥ 40) are indicated at each node. Scale bar corresponds to amino acid
627 substitutions per site. The sequence obtained from our samples is coloured in red.

628

629 **Table 1:** Information on sample collection.

630

631 **Table 2:** Information on the five viral genomes reconstructed from mosquito viromic data.

632

633 **Supplementary table 1:** Viral genomes that were reconstructed from mosquito viromic data,
634 including partial genomes that were not deposited into GenBank database.

635

636 **Supplementary table 2:** Contingency table which was used for statistical analyses.

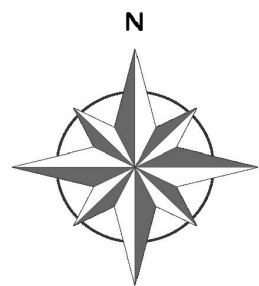
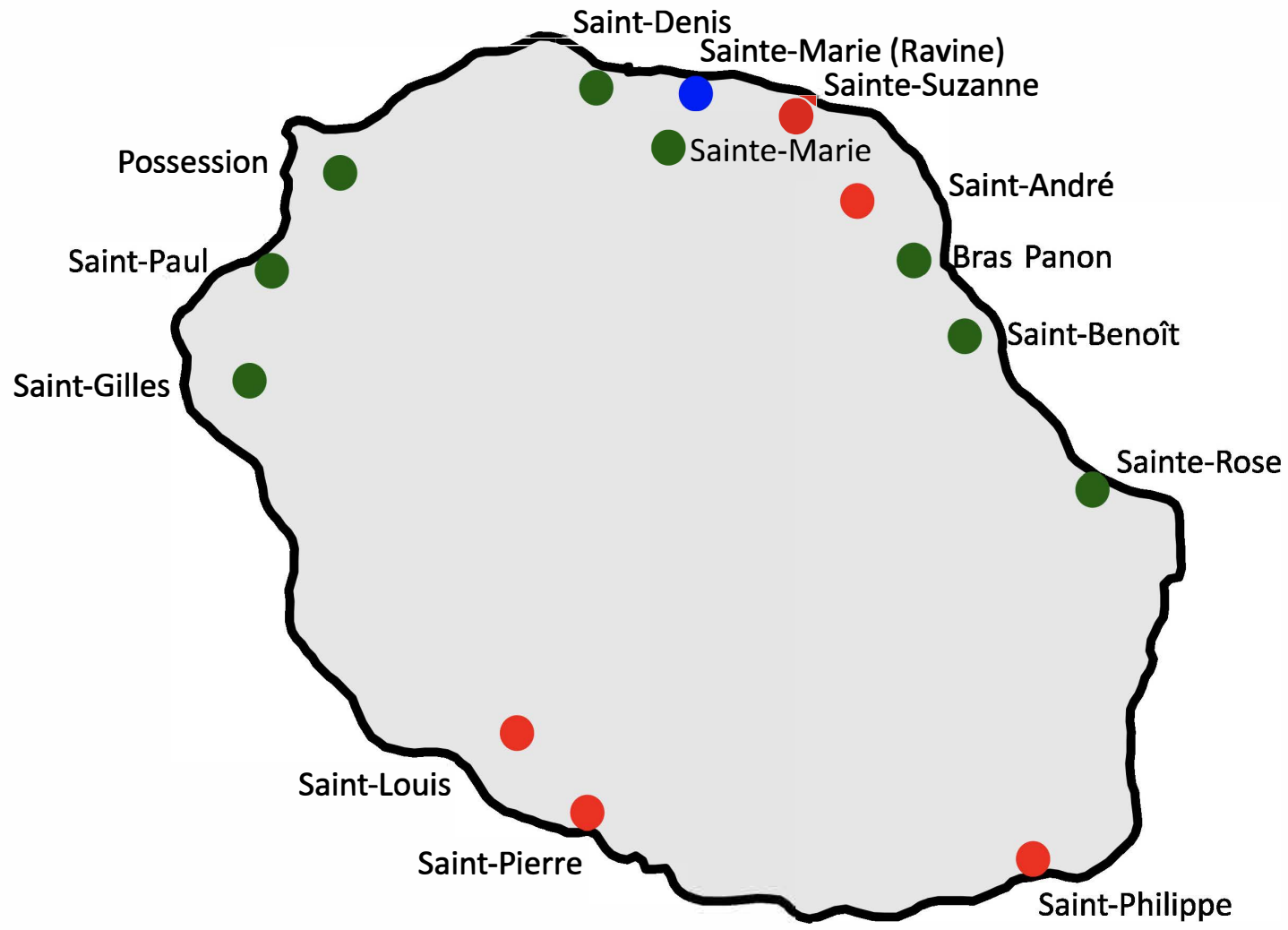
637

638 **Supplementary figure 1:** Diversity analysis of *Aedes albopictus* and *Culex quinquefasciatus*
639 viral communities at the family level. Boxplots indicate the observed numbers, Shannon
640 diversity and Simpson diversity (left to right). Pairwise comparisons were conducted using
641 Wilcoxon tests. The numbers indicate p values.




642

643

Figure 1



Mosquitoes species

-  *Aedes albopictus*
-  *Aedes albopictus* and *Culex quinquefasciatus*
-  *Culex quinquefasciatus*

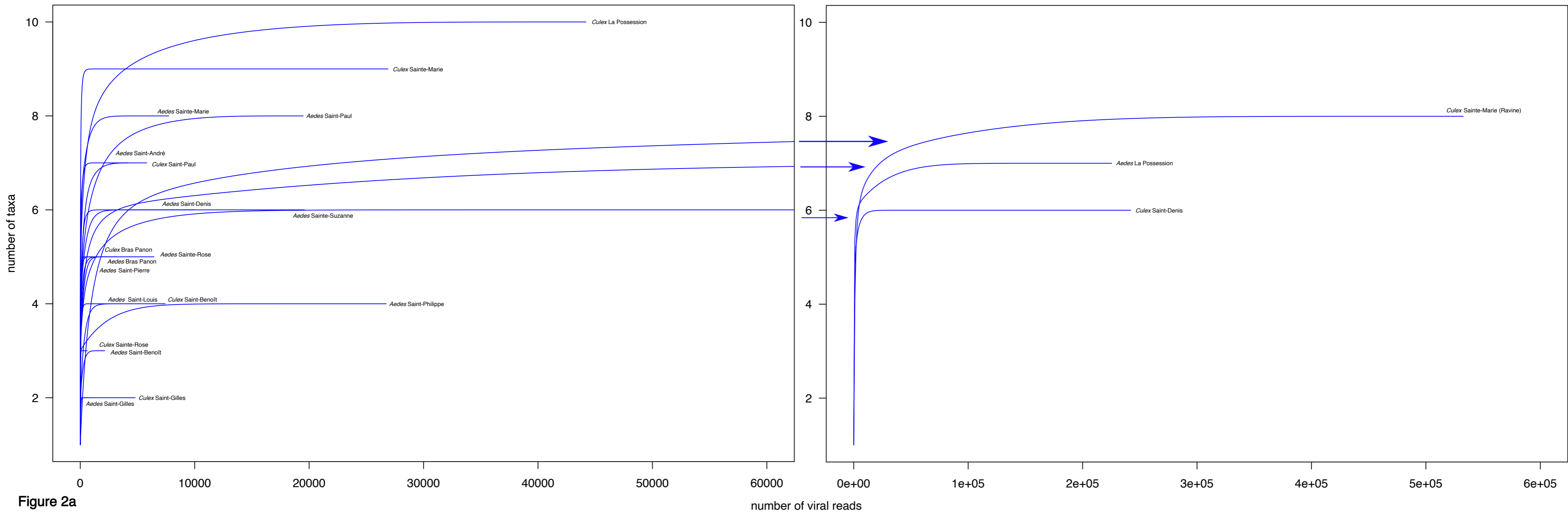


Figure 2a

Figure 2b

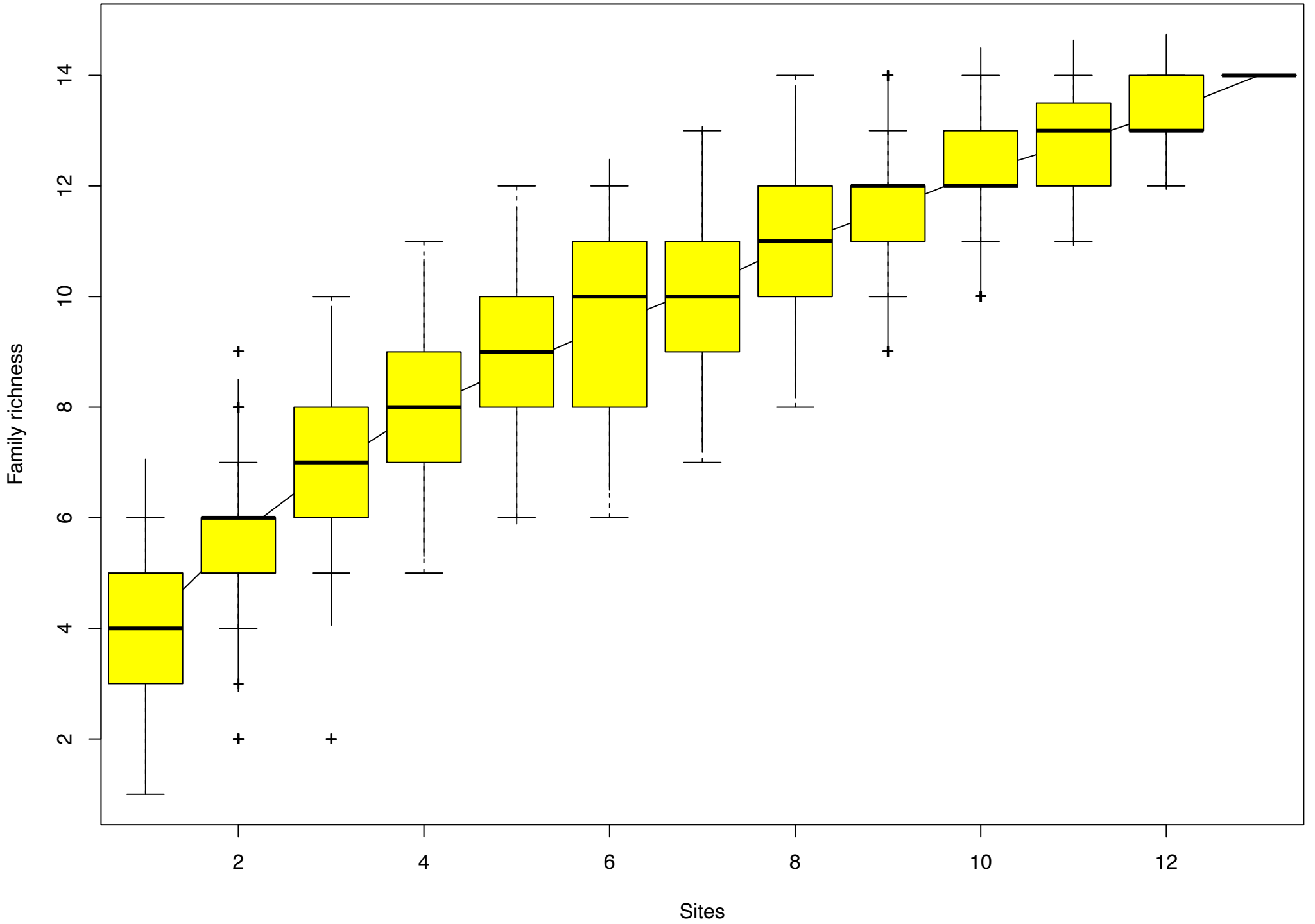


Figure 3

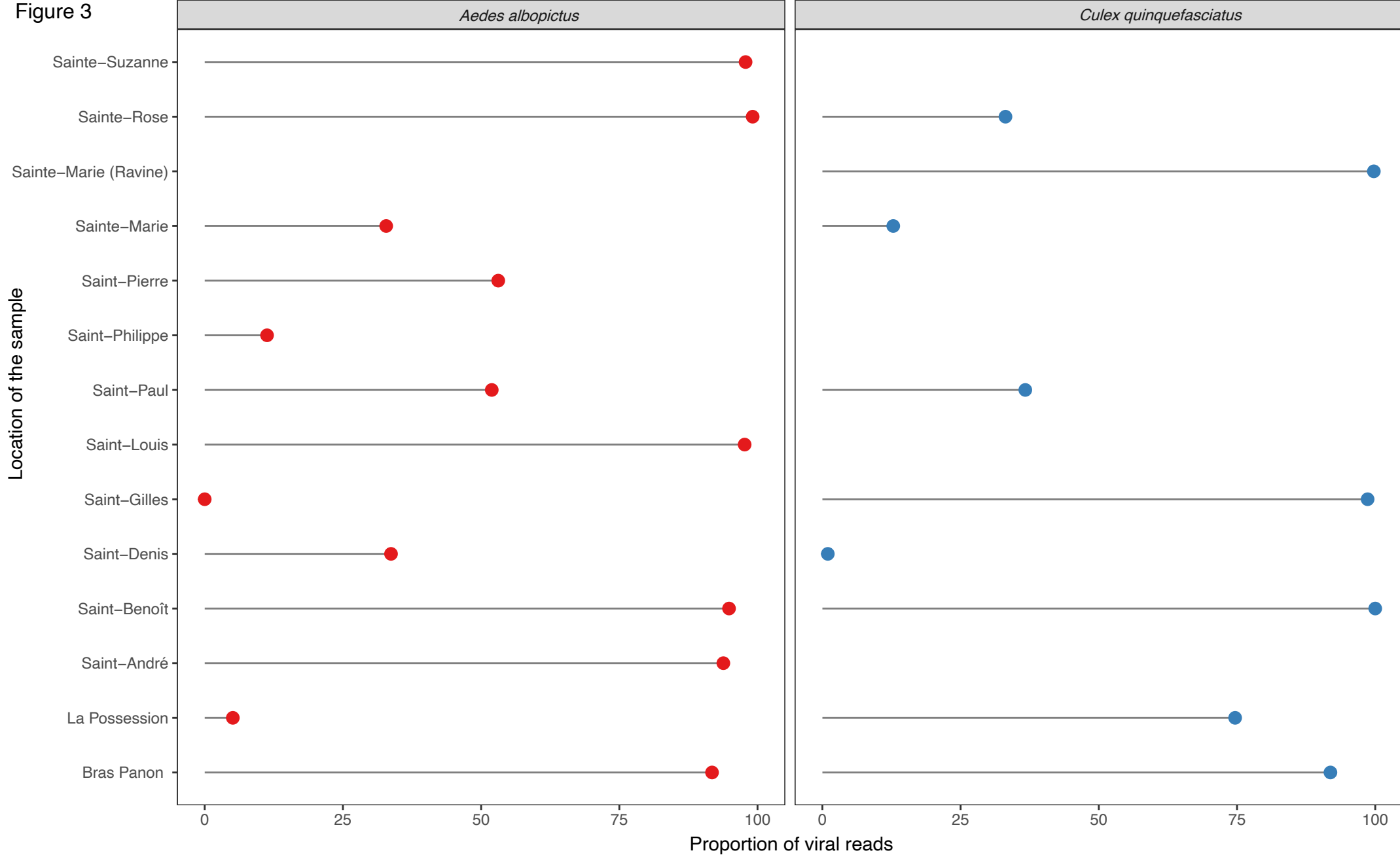


Figure 4

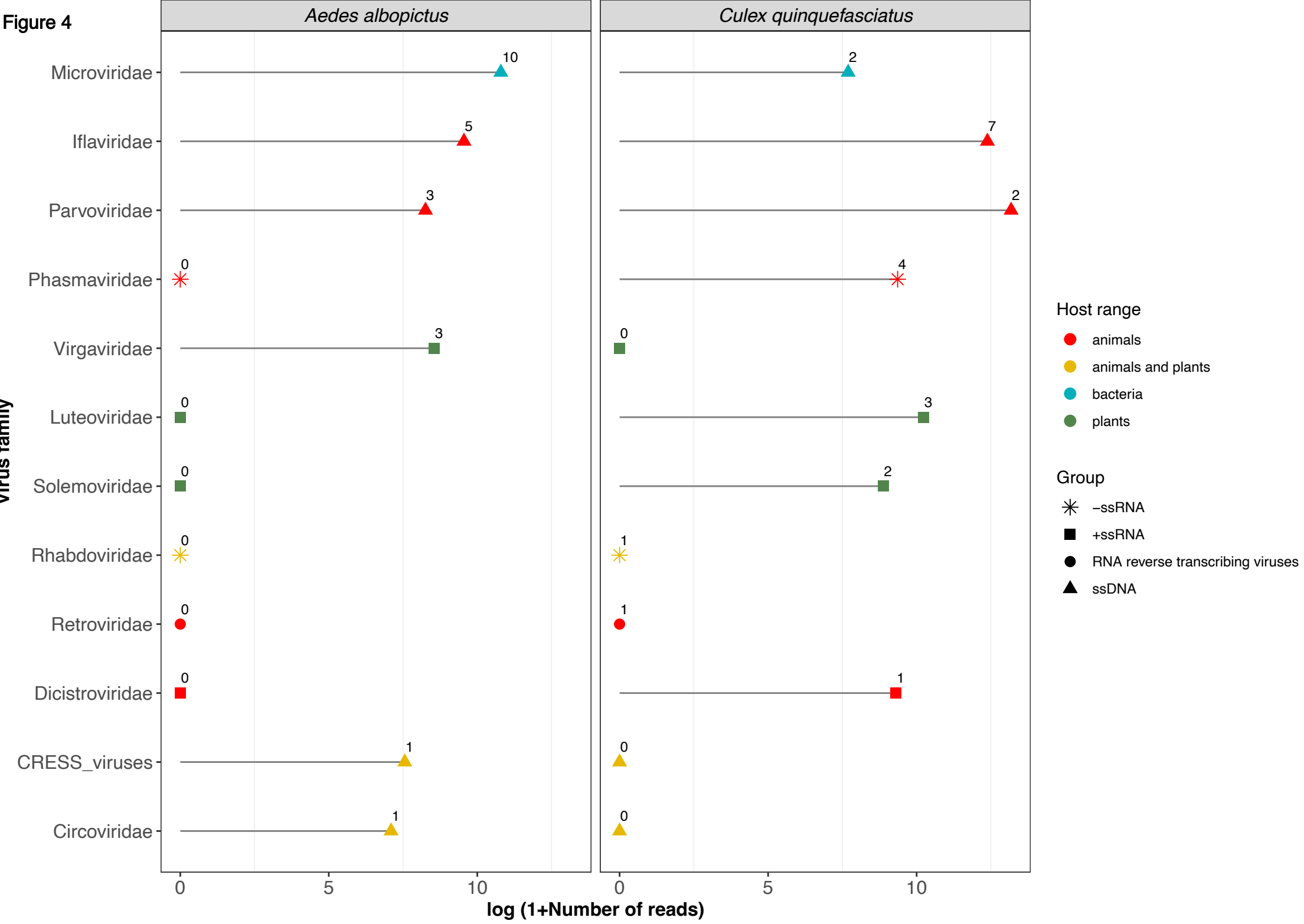


Figure 5

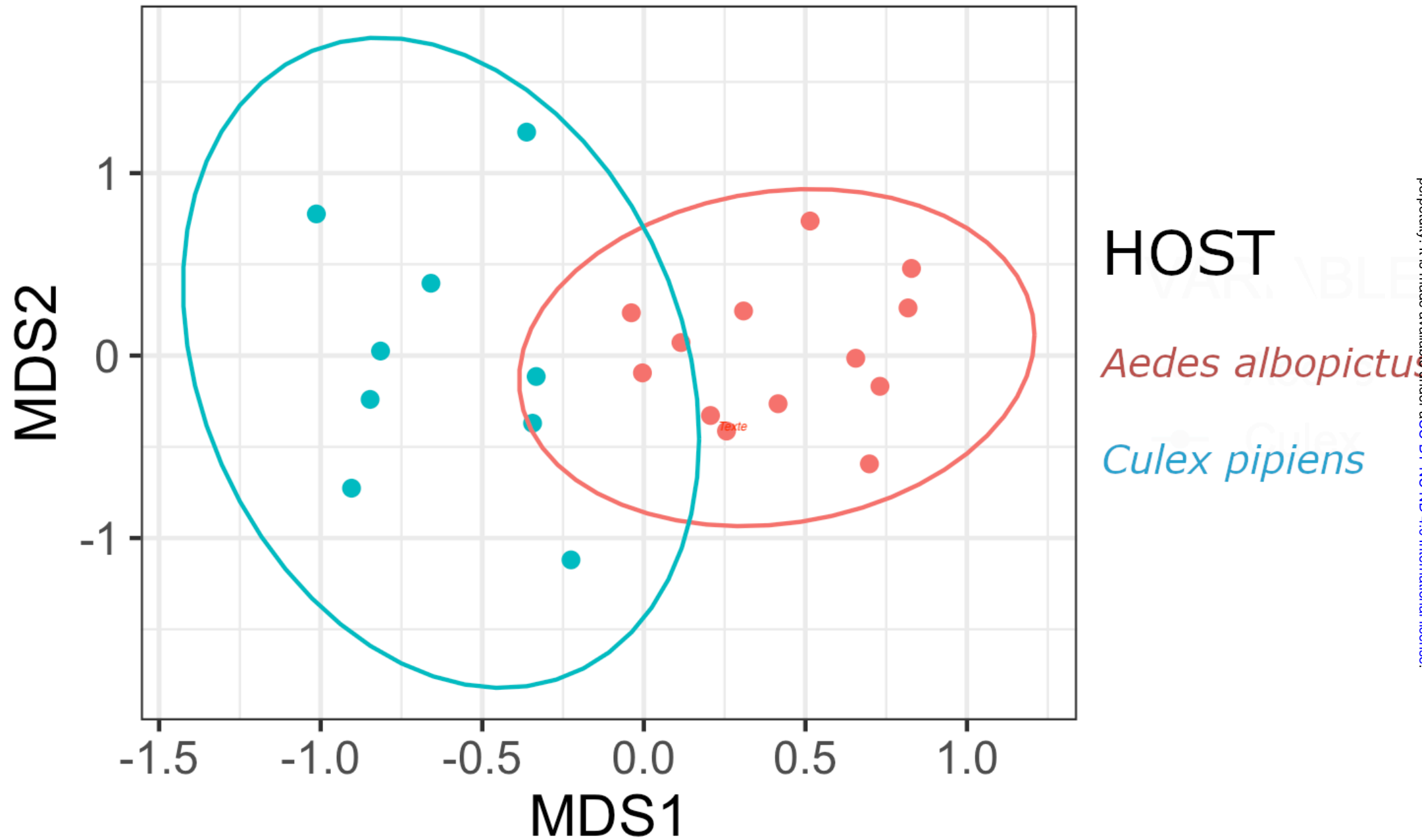
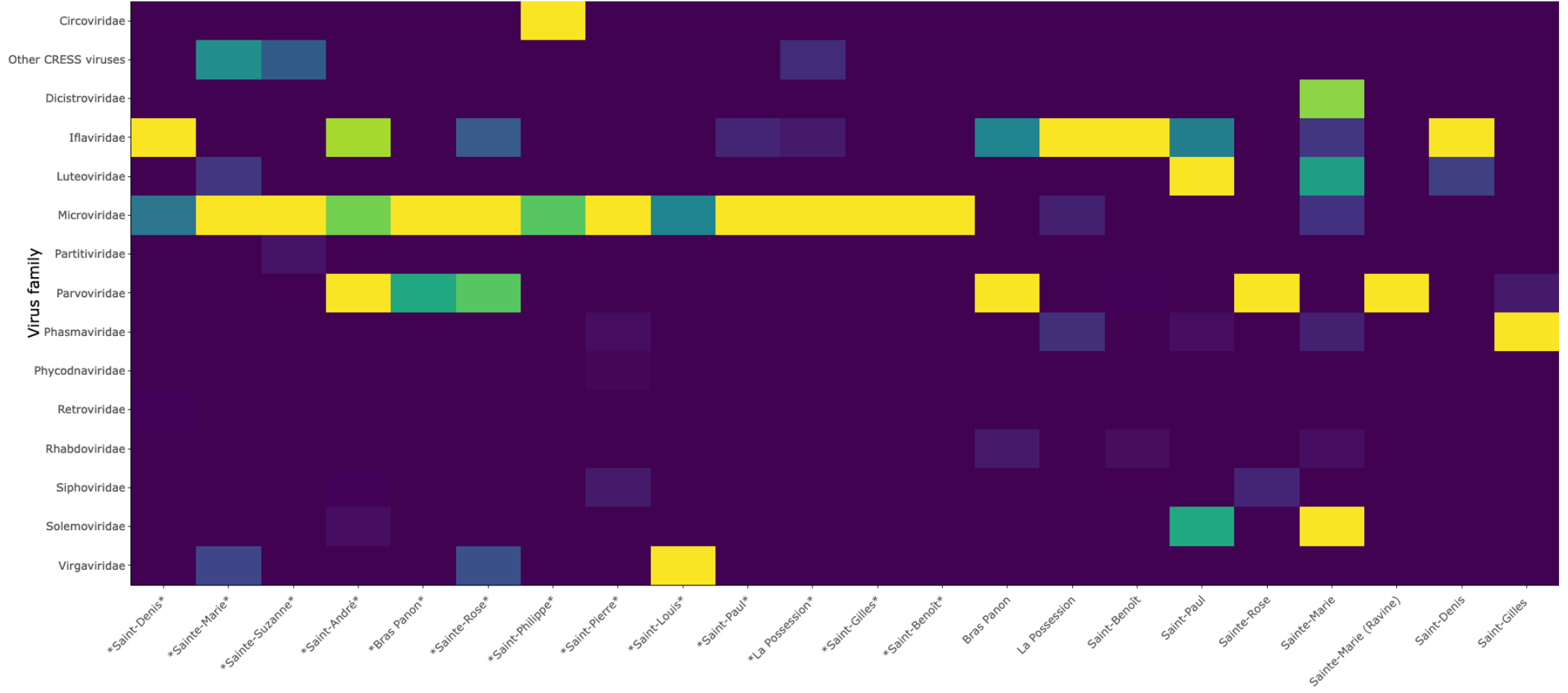
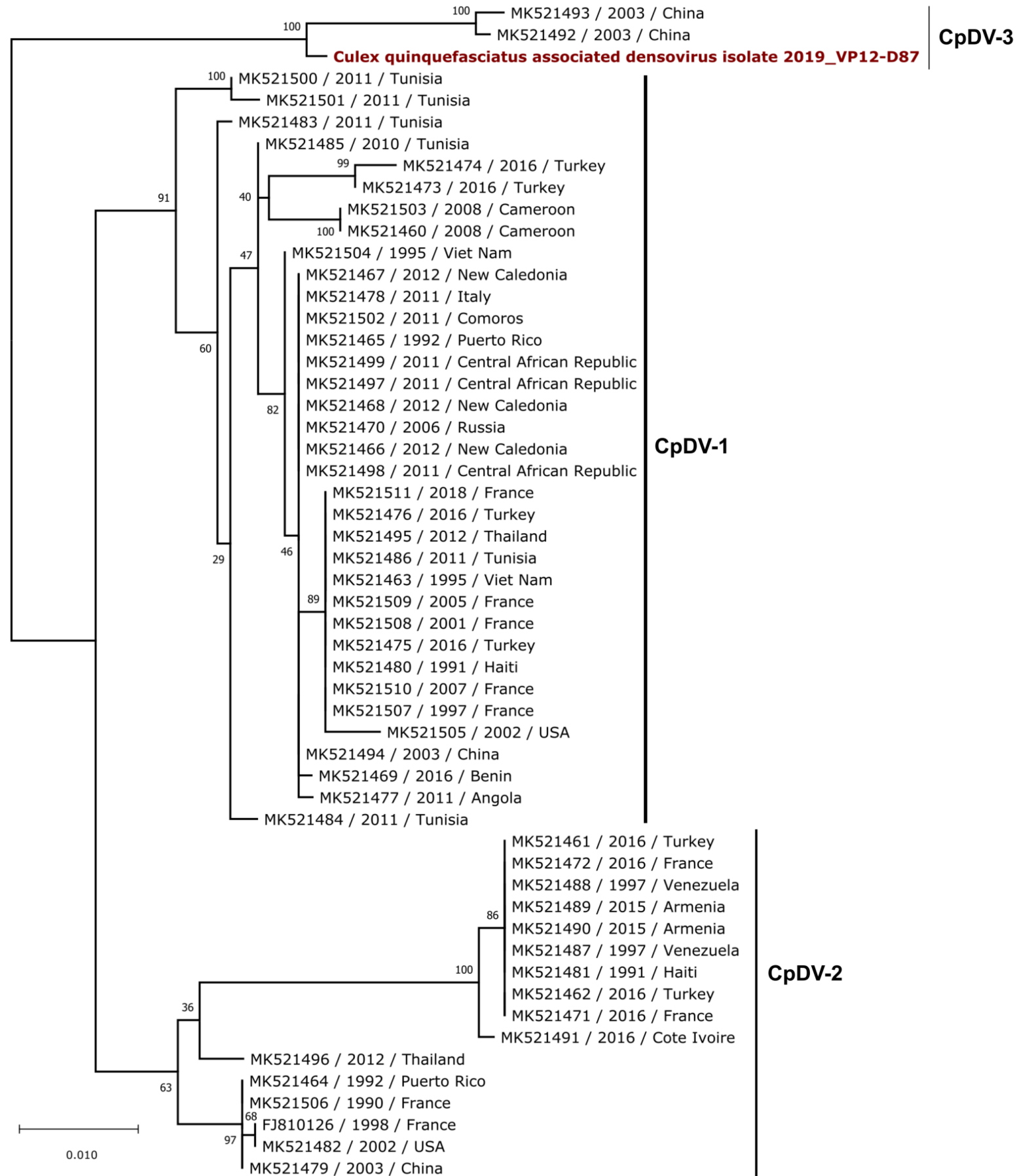


Figure 6





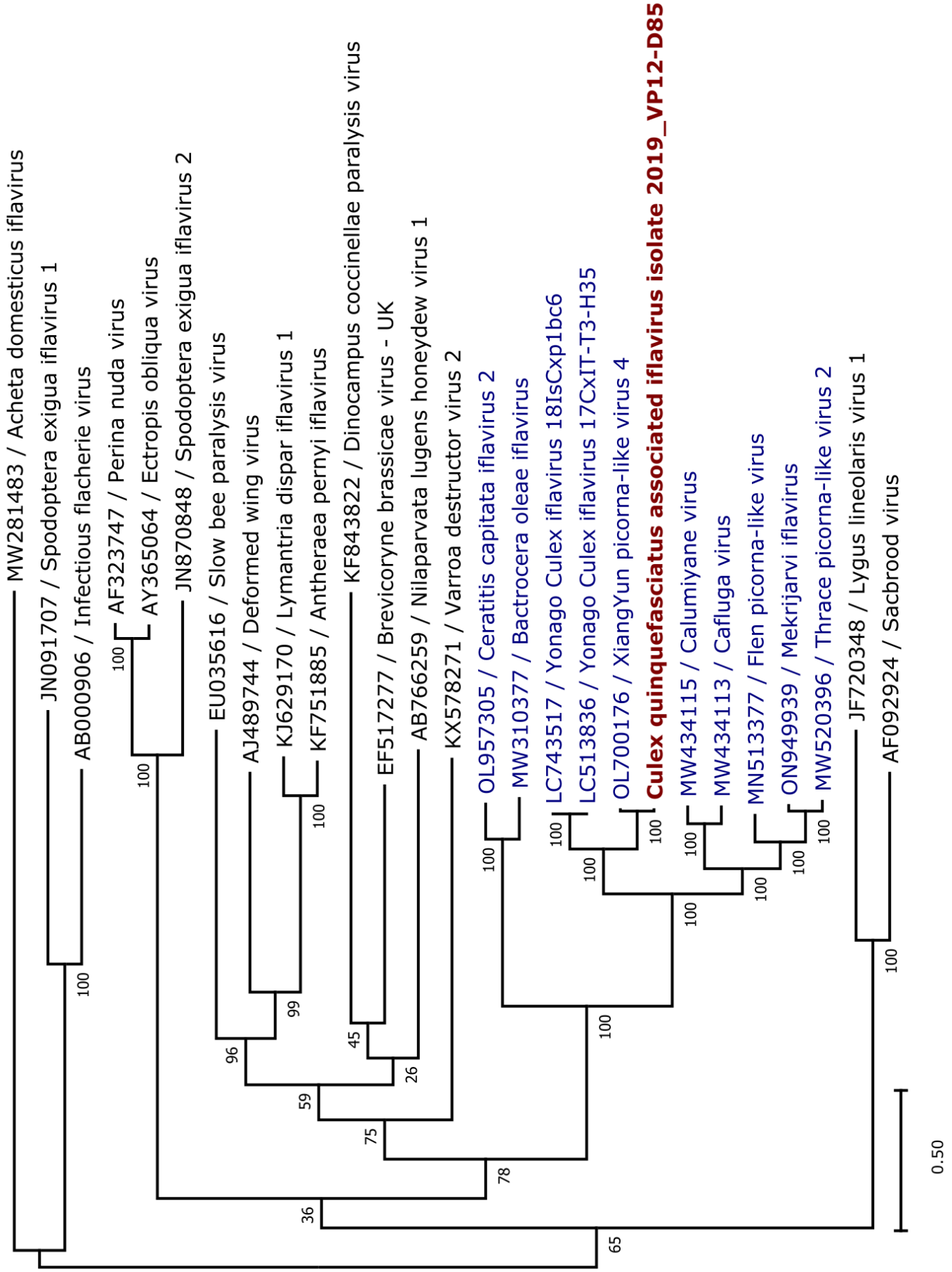


Figure 8

Figure 9

bioRxiv preprint doi: <https://doi.org/10.1101/2024.11.08.622592>; this version posted November 9, 2024. The copyright holder for this preprint (which was not certified by peer review) is the author/funder, who has granted bioRxiv a license to display the preprint in perpetuity. It is made available under a [CC-BY-NC-ND 4.0 International license](https://creativecommons.org/licenses/by-nc-nd/4.0/).

